Article

Experimental Study of Creep Acoustic Emission Characteristics of Coal Bodies around Boreholes under Different Moisture Contents

Tianjun Zhang [1,*] , **Zhiqiang Ling** [1,2], **Mingkun Pang** [1] **and Yukai Meng** [1]

1 College of Safety Science and Engineering, Xi'an University of Science and Technology, Xi'an 710054, China; lingzhq@163.com (Z.L.); 19120089022@stu.xust.edu.cn (M.P.); 13259795565@163.com (Y.M.)
2 Shaanxi Administration of Coal Mine Safety, Xi'an 710018, China
* Correspondence: tianjun_zhang@xust.edu.cn

Abstract: Water content is an important factor in the deformation-destruction process of coal bodies. To analyze the influence of water on the creep acoustic emission (AE) characteristics of coal rock surrounding a borehole, we conducted graded loading creep AE tests of single-hole specimens with different water contents (0%, 4%, 8% and water-saturation) under uniaxial loading. The findings include the following: the water content affects the creep mechanical properties of the coal body around a borehole. The creep transient strain and steady-state strain increased exponentially with rising water content; the saturated specimen showed the highest increase, reaching 44.5% and 28.6%, respectively. The specimen water content affected the cumulative ringing count (CRC) and the axial strain during creep. The axial strain increased with rising water content, the CRC increased linearly with rising axial strain. The higher the water content, the greater the CRC rise. At different stress levels, the CRC in the 4%, 8% and saturated water content specimens changed by 43%, 53% and 74%, respectively. The AE ringing rate showed a pattern of grow–decline–stabilize at each creep stage. The AEs decreased significantly with the rising water content and the creep curve lagged behind the AE data. This paper provides guidelines for gas extraction, borehole maintenance and AE detection.

Keywords: creep test; porous coal body; water content; cumulative ringing count; energy

1. Introduction

Creep deformation of a coal seam extraction borehole is one of the main causes of borehole instability deformation. After the drilling operation is completed, the coal body around the hole will continuously deform with time, and the composition and structure of the coal will be changed over time by the physical, chemical and mechanical action of groundwater [1,2]. Long-term submergence of the coal body increases the water content, which reduces its bearing capacity and strength, or even destroys it [3]. This affects its macroscopic mechanical properties, and the gradual accumulation of coal body damage will eventually affect the creep deformation properties of the coal body [4–6]. The creep properties of pore-bearing coal bodies differ from those of intact coal bodies; however, few studies have investigated creep deformation of coal bodies around boreholes [7–9]. Therefore, the study of the creep deformation process of coal body around the borehole is quite important for the application of gas extraction technology.

With the increasing research into coal bodies, more sophisticated instruments have been used for macroscopic studies [10–12]. The acoustic emission (AE) technique is an effective tool to detect the extension and expansion of microfractures in coal rock. The changes in the acoustic emission parameters obtained by this technique can reflect the changes in the internal structure of a coal rock body around a borehole when creep deformation occurs [13–15]. Chen et al. [16] conducted acoustic emission tests on samples with different moisture contents under uniaxial compression loading. This process concluded that the weakening of the peak stress and strength, elastic, strain, and the post-peak

modulus decreased to some extent with increasing moisture content and loading rate. To understand the weakening characteristics of coal induced by different water content levels, Qian et al. [17] tested coal samples with different water contents and found that the acoustic emission phenomenon was relatively obvious for fully saturated and non-saturated coal specimens. In the process of exploring the main factors affecting water–rock interaction, Heggheim et al. [18] analyzed the softening behavior of sandstone by analyzing the sandstone grain variation, pore morphology and pore size. To study the effect of water content on critical and breaking strains, Daraei et al. [19] carried out uniaxial compressive strength tests on 67 specimens of eight rock types under dry, natural and saturated conditions and showed that the changes in the critical and breaking strains occurred mainly at water contents below 2%. Qin et al. [20] measured the acoustic emission characteristics of square coal samples with different water contents under uniaxial compression, and compared the stress–strain characteristics and damage evolution of the coal samples. The effects of water content on coal's permeability properties, mechanical properties and energy dissipation were analyzed by Jing et al. [21], Wei et al. [22] and Jiang et al. [23] using self-designed experimental platforms. The above studies only investigated the acoustic emission phenomena, and rarely studied the acoustic emission characteristics from the perspective of creep deformation of the coal body around the borehole, and then analyzed the relationship between the water content, creep strain and acoustic emission characteristic parameters.

In this paper, creep acoustic emission tests were carried out on hole-containing specimens with different water contents to analyze the effect of water content on creep mechanical behavior and the acoustic emission parameters of coal samples. The paper results show the temporal sequence law of coal creep deformation around a borehole, which can provide important guidance for gas extraction, borehole support and acoustic emission detection.

2. Rock Creep Model

The creep damage model can effectively reveal the material creep mechanism and creep process from multiple perspectives. It consists mainly of elastic, viscous, and plastic elements connected in series and parallel [24,25]. Creep deformation of the coal body around the hole is a phenomenon in which the deformation of the coal body becomes larger with time under the condition that the stress remains constant.

According to the characteristics of some creep curves, the model established needs to reflect the mechanical characteristics of the elastic strain phase, deceleration creep phase, steady creep phase and accelerated creep phase [26,27]. Most scholars describe the creep process utilizing the Nishihara model (Figure 1), where I is a Hooker body, II is a Kelvin body, and III is a viscoplastic body. The σ is the applied stress, and the σ_s is the stress at which the material reaches the damage state. The E_0 is the modulus of elasticity of the Hooke body. The E_1 and η_1 are the modulus of elasticity and the coefficient of viscosity of the Kelvin body, respectively. The η_2 is a viscous coefficient in a viscoplastic body.
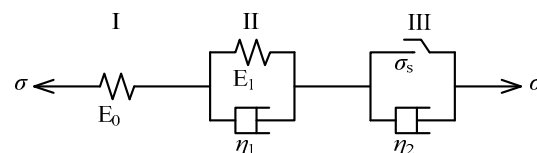

Figure 1. The Nishihara model.

This model satisfies the following intrinsic structure relations:

$$\varepsilon = \begin{cases} \frac{\sigma}{E_0} + \frac{\sigma}{E_1}[1 - \exp(-\frac{E_1}{\eta_1}t)], & \sigma < \sigma_\text{s} \\ \frac{\sigma}{E_0} + \frac{\sigma}{E_1}[1 - \exp(-\frac{E_1}{\eta_1}t)] + \frac{\sigma - \sigma_\text{s}}{\eta_2}t, & \sigma_\text{s} \le \sigma \end{cases} \tag{1}$$

Of course, the Nishihara model better reflects the mechanical properties of decelerating creep and steady creep of the material, but cannot account for the mechanical properties

of the accelerated creep phase of the specimen containing pores; therefore, the authors improved the Nishihara model by adding a viscoplastic element that reflects the accelerated creep phase. Additionally, we established the damage creep intrinsic model considering different factors. For the convenience of presentation, it is named the NVPE model. The basic model is shown in Figure 2.
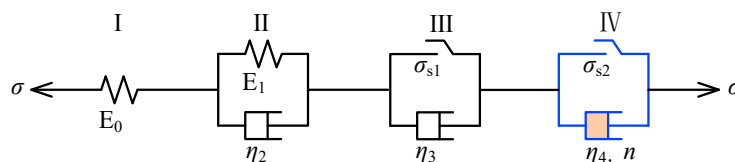

Figure 2. Improved Nishihara model.

Here, E_0 and E_1 are the modulus of elasticity of the specimen, MPa. η_2, η_3 and η_4 are the coefficient of viscosity for elements II, III and IV, respectively, σ_{s1} and σ_{s2} are the long-term strength and yield strength of the specimen, MPa, respectively, where $\sigma_{s1} < \sigma_{s2}$, and n are the creep coefficients of the specimen. Element I represents the deformation process of the coal rock material when loaded, II represents the deceleration creep stage of the coal rock material, III represents the stable creep stage of the coal rock material, and element IV represents the accelerated creep stage of the coal rock material.

The improved one-dimensional creep equation for the Nishihara model is:

$$\varepsilon = \begin{cases} \frac{\sigma}{E_1} + \frac{\sigma}{E_2}\left(1 - e^{-E_2/\eta_2 \cdot t}\right), & \sigma < \sigma_{s1} \\ \frac{\sigma}{E_1} + \frac{\sigma}{E_2}\left(1 - e^{-E_2/\eta_2 \cdot t}\right) + \frac{\sigma - \sigma_{s1}}{\eta_3}t, & \sigma_{s1} \leq \sigma < \sigma_{s2} \\ \frac{\sigma}{E_1} + \frac{\sigma}{E_2}\left(1 - e^{-E_2/\eta_2 \cdot t}\right) + \frac{\sigma - \sigma_{s1}}{\eta_3}t + \frac{\sigma - \sigma_{s2}}{\eta_4}t^n, & \sigma_{s2} \leq \sigma \end{cases} \tag{2}$$

From the above equation, it can be seen that when its stress is less than the long-term strength, the creep expression for a large enough creep time is:

$$\varepsilon = \lim_{t \to \infty}\left(\frac{\sigma}{E_1} + \frac{\sigma}{E_2}\right) \tag{3}$$

When the stress is greater than the long-term strength, the creep expression is:

$$\varepsilon = \lim_{t \to \infty}\left(\frac{\sigma}{E_1} + \frac{\sigma}{E_2}\right) + \frac{\sigma - \sigma_{s1}}{\eta_3}t \tag{4}$$

When the stress is greater than the yield strength, the creep expression is:

$$\varepsilon = \lim_{t \to \infty}\left(\frac{\sigma}{E_1} + \frac{\sigma}{E_2}\right) + \frac{\sigma - \sigma_{s1}}{\eta_3}t + \frac{\sigma - \sigma_{s2}}{\eta_4}t^n \tag{5}$$

The change in the modified Nishihara creep model curve before and after the long-term strength of the material is reached shows that when the loading stress is less than the long-term strength, the creep rate in the stable creep phase is 0. When the applied stress is higher than the long-term strength and lower than the breaking strength, the rate of stable creep of the material is the ratio of the applied stress minus the long-term strong stress to the coefficient of viscosity in the Bingham body. When the loading stress is greater than the yield stress, the accelerated creep phase appears; with time, the creep deformation rate gradually increases, and the accelerated creep characteristics are significant.

3. Experiments

In engineering, the gas extraction rate of loose coal seam is generally low and the stability of the borehole is poor. Therefore, it is important to study the deformation-destruction characteristics of loose coal samples for gas extraction. However, it is difficult

to take samples of loose coal, so similar materials are chosen as the base materials of the specimens, and the mechanical parameters of the specimens obtained from the tests can meet the test requirements.

3.1. Material Preparation

3.1.1. Sample Preparation

In order to test the strength parameters of such loose coal bodies, we researched the relevant parameters of the coal in several mining areas and selected suitable matching materials for the tests. The main steps include the test specimens that were created from a mixed slurry of coal dust, gypsum, and cement with a mass ratio of 1:0.5:1. The slurry was poured into a $70 \times 70 \times 140$ mm molds, and a long cylindrical body representing the drilling device was placed in the center of the box to simulate the borehole; it was removed after the specimens were dried. The specimens are shown in Figure 3.
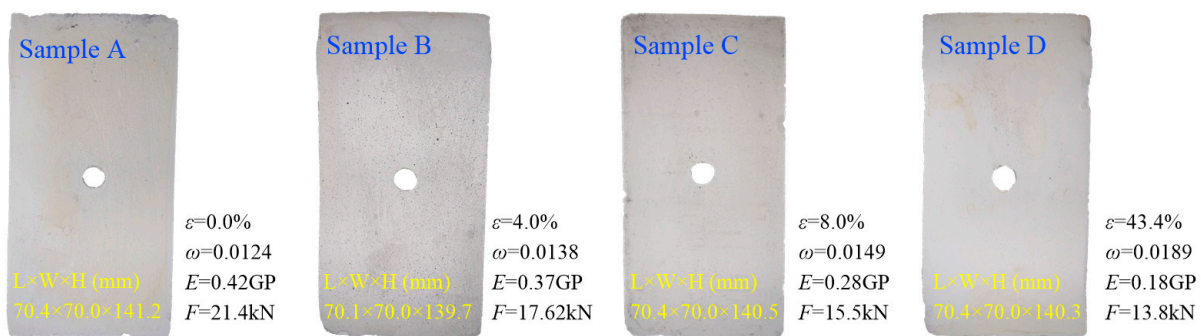

Figure 3. The four specimen groups with their physical parameters.

The air-dried specimens were divided into four groups: A, B, C, and D, with six samples in each group. Group A was the dry group, groups B and C were the controlled water-content group, and group D was the naturally water-saturated group. Control of the water content, group specimen water content, and the specimen were placed in a constant temperature and humidity box. Natural saturated water content groups are placed in a closed water container to control the liquid surface from the top surface of the specimen 30~40 mm, in a cool place to stand for 24 h after weighing, and is weighed every 24 h until the weight of the specimen is stable, and the quality of the specimen is recorded.

3.1.2. Basic Parameters

In the field, when water is injected into a borehole at the underground working face, the coal seam is usually in a completely submerged environment, and the coal body around the borehole is water-saturated. In time, the saturation reaches a natural balance whereby the greater the distance from the borehole, the lower the water content of the coal body. Therefore, for the modeling in this paper, we prepared four specimen groups, A, B, C and D, with different water contents: 0%, 4%, 8%, and natural saturation, respectively, representing the natural variation in the water content of the coal seam after water injection. Each group comprised six specimens.

Among the 24 specimens containing holes, A_i, B_i, C_i, D_i ($i = 1, 2, 3$) were used for the uniaxial compressive damage test, and A_i, B_i, C_i, D_i ($i = 4, 5, 6$) were used for the graded creep loading test. The basic parameters of the specimens, as derived from the uniaxial compressive test, are shown in Table 1.

Table 1. Basic parameters of specimens derived from uniaxial compressive test.

Number	Average Moisture Content w/%	Peak Axial Strain ε	Modulus of Elasticity E/GPa	Peak Intensity P/MPa	Peak Load F/kN
A1		0.0124	0.415	4.358	21.352
A2	0.0	0.0118	0.411	4.237	20.761
A3		0.0132	0.424	4.443	21.772
B1		0.0138	0.372	3.597	17.624
B2	10.4	0.0134	0.366	3.438	16.847
B3		0.0125	0.364	3.399	16.655
C1		0.0149	0.275	3.167	15.516
C2	19.3	0.0148	0.277	3.136	15.371
C3		0.0155	0.283	3.309	16.213
D1		0.0189	0.187	2.814	13.791
D2	28.4	0.0191	0.188	2.854	13.987
D3		0.0182	0.182	2.615	12.812

3.2. Methodologies

3.2.1. Experiment Design

The experiments were carried out in the mechanics laboratory of Xi'an University of Science and Technology, China. The loading system for this test was the YYL200 electronic persistent creep tester (CRIMS, Jilin, China). The YYL200 tester loading range is 0–200 kN and the loading rate is 0.01–80 mm/min. The graded loading test designed in this paper can observe the loading deformation and constant load deformation under different stress levels at the same time, so the test conditions are in the graded loading mode. We set a loading time of 10 min and a constant load time of 120 min for each phase. The SAEU2S acoustic emission equipment is produced by BJSHXY Technology Co., Ltd., Beijing, China. The system includes a transducer, preamplifier, data acquisition card and computer. The gain of the preamplifier is 40 dB. The acquisition frequency was 10,000 kHz, and the threshold value was set to 40 dB. The acoustic emission test system is shown in Figure 4.
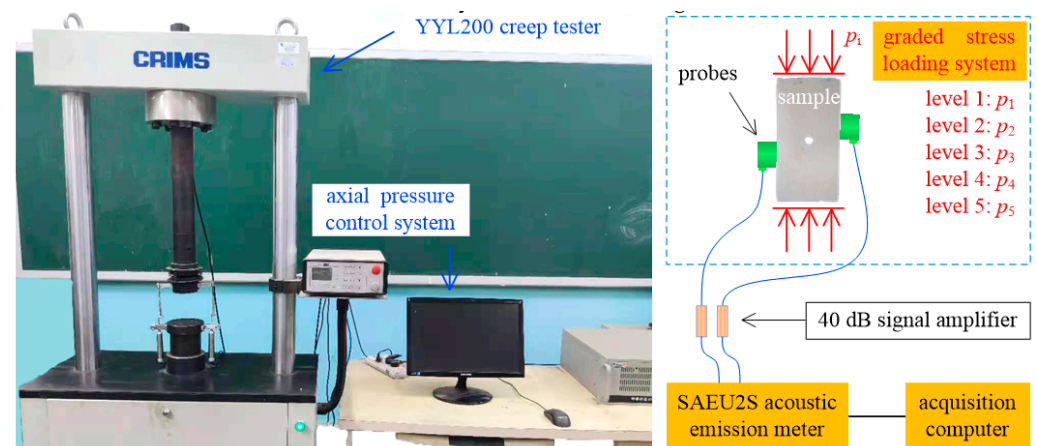
Figure 4. Acoustic emission test system.

3.2.2. Experiment Design

According to the average uniaxial compression test results, we took 50%, 60%, 70%, 80% and 90% of the peak stress as the creep test loading levels of the five stress levels. The axial load, stress level, loading time and constant loading time settings for each level of the graded loading creep test are shown in Table 2.

Table 2. Loading parameters at each level of graded loading for uniaxial compression test.

Group	Water Content/%	Stress Level	Axial Load/kN	Stress Level/MPa	Group	Water Content/%	Stress Level	Axial Load/kN	Stress Level/MPa
A	0.0	level 1	10.65	2.17	C	19.3	level 1	7.85	1.60
		level 2	12.78	2.61			level 2	9.42	1.92
		level 3	14.91	3.04			level 3	10.99	2.24
		level 4	17.04	3.48			level 4	12.56	2.56
		level 5	19 17	3.91			level 5	14.13	2.88
B	10.4	level 1	8.52	1.74	D	28.4	level 1	6.77	1.38
		level 2	10.23	2.09			level 2	8.12	1.66
		level 3	11.93	2.43			level 3	9.47	1.93
		level 4	13.63	2.78			level 4	10.82	2.21
		level 5	15.34	3.13			level 5	12.18	2.49

4. Results and Discussion

The coal rock body around a gas extraction borehole is affected by water–stress coupling; in this setting a drilled coal body can be damaged more easily than an intact coal rock body. This occurs because drilling disturbs the stress equilibrium state of the intact coal rock, forcing the redistribution of stress around the borehole, which weakens the coal rock body. Therefore, in this paper, the following analyses were performed for coals with different moisture contents, the main parameters included: creep displacement, calculation of strain, acoustic emission parameters, etc.

4.1. Effect of Moisture Content on the Creep Process of Specimens

In the graded loading test scheme, the graded creep test of the laboratory specimens with different moisture contents was carried out at room temperature (35–40 °C). Because of the variation in the quality of the specimens due to the preparation process, some deviation in the test results was expected. Therefore, the test parameters of each group of specimens were taken as their average values, and the strain change histories of specimens with different moisture contents were obtained (Figure 5).

(**a**) 0.0% moisture content group

(**b**) 4.0% moisture content group

(**c**) 8.0% moisture content group

(**d**) 43.4% moisture content group
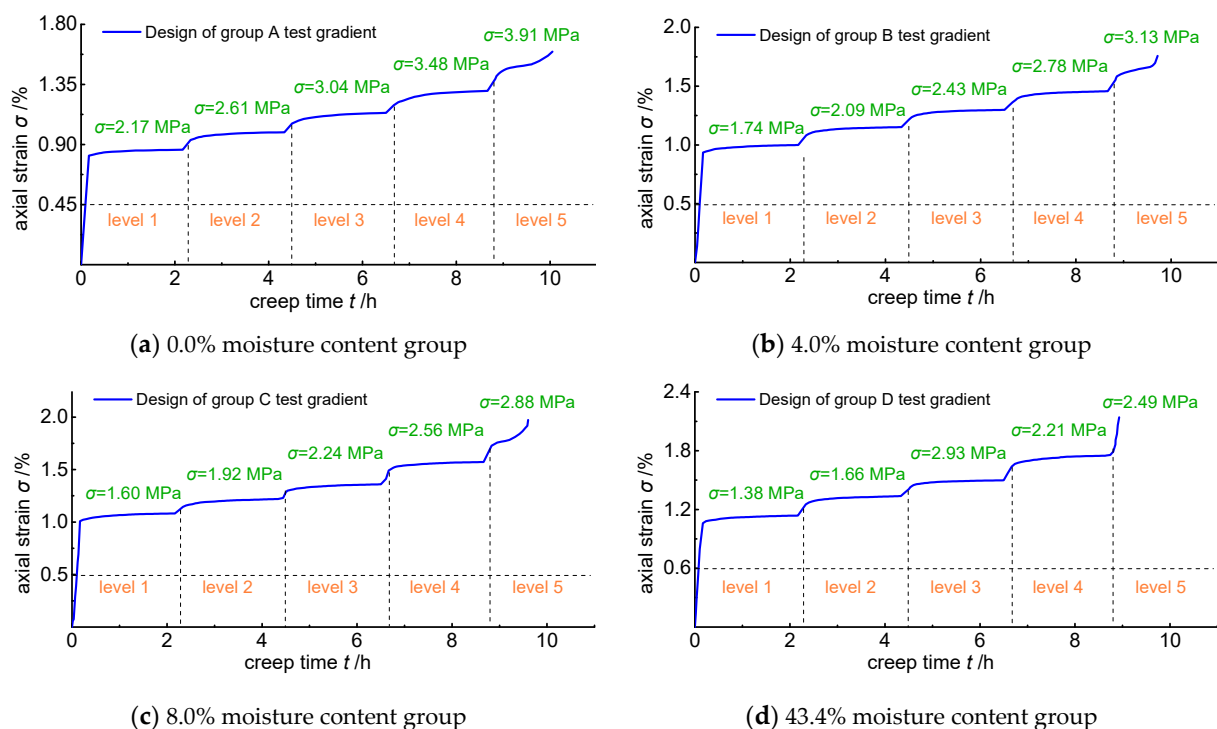
Figure 5. Strain variation curves of specimens with different water content.

The results show that as the water content increased, the axial strain of the specimen increased, with a maximum axial strain of 1.36%, 1.41% and 1.47% for the specimens with 0.0%, 4.0% and 8.0% water content, respectively, and 1.75% increase for the saturated specimen. The maximum axial strain for the saturated specimens increased by 28.67% compared to that of the dry specimens.

The creep curves of Figure 5 also show that the four groups of specimens were not deformed and damaged within the range of 50% to 80% of their peak stresses; the curves showed only two stages of creep at each level: decay creep and stable creep. Moreover, the creep curve value of the dried specimen is the smallest, below all the curves, and its curve tends to rise with the increase in water content.

Water can moisten the particles on the free surface of the coal body, reducing the cohesion between the particles. This changes the mechanical properties of the coal body, making the coal body around the hole more easily deformed by external forces. Thus, water can have a great influence on the strength of the pore-bearing coal samples, mainly in the amount of axial strain and displacement during loading.

4.2. Calculating the Transient and Steady-State Strains of the Specimens

Creep properties refer to the variation of strain of a material with time. For the analysis of creep processes in coal bodies, both transient creep and steady-state strain are generally considered. These two calculation methods are described in detail in the following section.

4.2.1. Instantaneous Strain Value Calculation Method

The instantaneous elastic strain variation laws of specimens with different moisture contents were fitted under the same stress level conditions. Analyzing the initial instantaneous strains of the four groups of specimens, we found that the instantaneous strains of the specimens gradually increased with the increment of the water content. The initial instantaneous strains in the first stage for the four moisture contents are 0.900×10^{-2}, 0.907×10^{-2}, 0.915×10^{-2} and 1.060×10^{-2}. The initial instantaneous strain at each stress level increases exponentially as the water content increases. The fitted equation for the dry specimens is $0.894 \times e^{(0.00391w)}$; the equation for the moisture content of 4.0% is $1.014 \times e^{(0.0044w)}$ and that for the moisture content of 8.0% is $1.141 \times e^{(0.005w)}$. The equation of the fitted curve for the saturated specimens is $1.308 \times e^{(0.052w)}$. All the fitting results showed high correlation, with correlation coefficients above 0.97.

These results indicate that as the water content increases, the strength and bearing capacity of the coal body around the hole will decrease. The larger the water content, the greater the water wedge effect on the coal rock under a continuous load, and the greater the initial deformation degree of the borehole. The relationship between steady-state strain and stress level is shown in Figure 6.
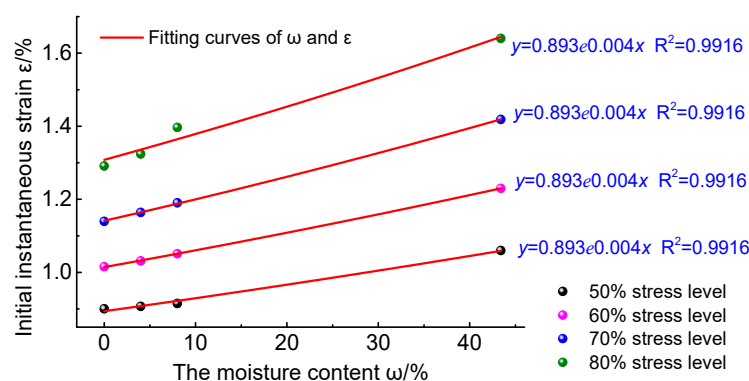

Figure 6. Initial instantaneous strain vs. water content fitting curve for various stress levels.

4.2.2. Calculation Method of Steady-State Strain

Steady-state strain is the strain (ε_w) in the uniform phase of the creep process of the specimen. Figure 7 shows the steady-state strain versus stress level and water content. The steady-state strain increases with rising stress level, and increases exponentially with the rising water content. At the same stress level, the increase in the steady-state strain in the saturated specimens was more significant. Taking the stress level of 80% as an example, the steady-state strain of the dry specimen was 1.339×10^{-2}, and when the water content increased to 4%, the steady-state strain increased to 1.389×10^{-2}, an increase of 3.7%. When the water content increased to 8%, the steady-state strain increased by 8.2%. For the saturated specimens, the steady-state strain increased by 28.6%.
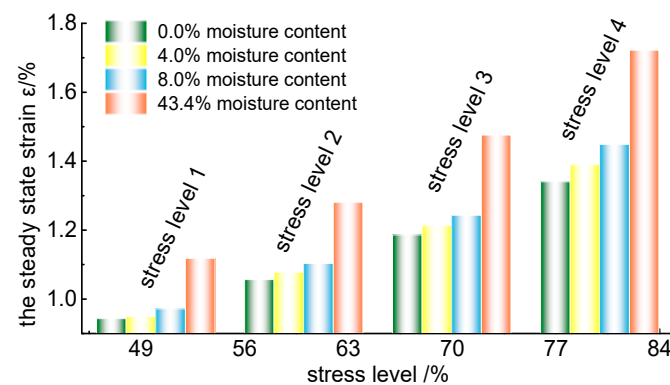

Figure 7. Steady-state strain versus stress level and moisture content.

The analysis shows that the presence of water accelerates the creep deformation of the borehole, and the steady-state strain of the perimeter coal body in the uniform creep stage increases with the increase of water content. The higher the water content, the greater the creep variation of the coal body into the uniform creep stage. In particular, the deformation of creep of the specimen is more obvious in the natural water-filled state, which is similar to the relationship between the conventional water content and the steady-state strain. Therefore, under the action of a continuous external force, the higher the water content, the greater the deformation produced by the coal rock around the borehole, and the phenomenon of destabilization is more likely to occur and collapse the borehole, so the study of the effect of different water content on the creep of the coal body around the borehole can provide guidance significance for gas extraction and borehole support.

4.3. Relationship between the Creep Process and the Ringing Count Rate

The creep process of perforated coal rock is accompanied by acoustic emission [13,14]. In order to further study the creep process of specimens containing pores, and the effect of water content on the acoustic emission pattern of specimens, this paper tests the acoustic emission characteristic parameters of specimens during the whole process of creep by using an acoustic emission test system. The acoustic emission ringing count rate curve is shown in Figure 8.

The acoustic emission ringing rate is significantly affected by the water content of the specimen. The dry specimens show the highest ringing rate at each loading stage and at the uniform creep stage. The acoustic emission activity was weaker in the specimens with water contents of 4%, 8% and 43.4%. The relative variation of creep acoustic emission ringing rate at each pressure level is small, but the ringing rate decreases with the increase in water content, and the decrease of different specimens is shown in Table 3. This is mainly due to softening of the specimen when the internal particles of the specimen react with the water. The higher the water content, the greater the degree of softening; hence, compared with the dry specimens, the water-saturated specimens experience less damage under loading and their acoustic emission ringing rate is lower (Table 3).
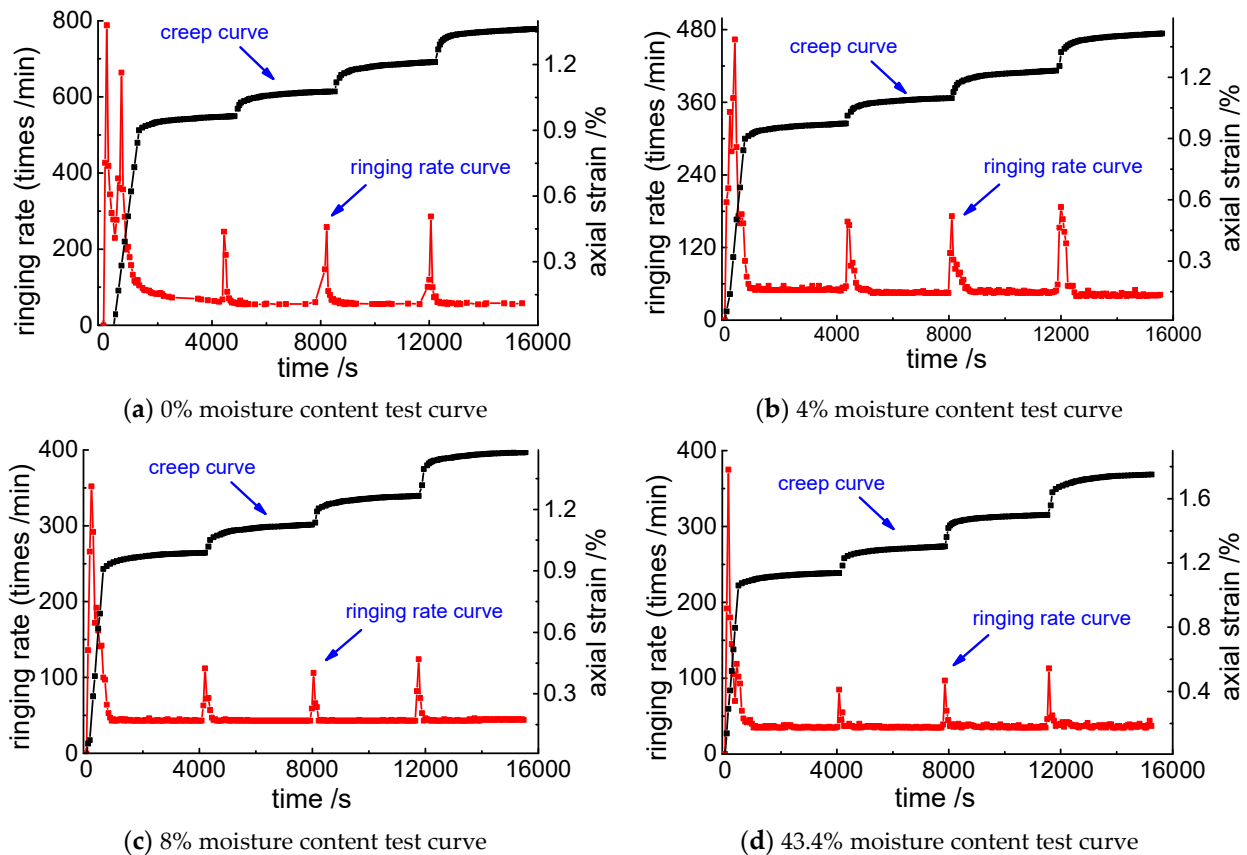
(**a**) 0% moisture content test curve

(**b**) 4% moisture content test curve

(**c**) 8% moisture content test curve

(**d**) 43.4% moisture content test curve

Figure 8. AE ringing count rate (red line) with increased axial strain (black line) for the four specimen groups.

Table 3. Acoustic emission ringing rate decline in the four specimen groups.

The Moisture Content/%	First Stage Ring Rate Drop/%	Second Stage Ring Rate Drop/%	Third Stage Ring Rate Drop/%	Fourth Stage Ring Rate Drop/%
0	90.7	77.2	78.3	79.7
4	82.2	71.2	73.3	77.5
8	77.6	62.1	60	63.2
43.4	72.4	59.1	63.9	64.6

During the loading process, the deceleration creep stage and the uniform creep stage of the creep process begin when the loading level for each stage is reached. In the deceleration creep stage, the specimen's internal fracturing expands and the acoustic emission activity increases. With increased loading, the acoustic emission ringing rate rises; the higher the water content, the lower the acoustic emission ringing rate. With the increased loading time, the acoustic emission ringing rate decreases accordingly. When the compression process of each specimen enters the uniform creep stage, the specimen has less new fracture development and the acoustic emission ringing rate shows a trend of first weakening and then leveling off compared with the deceleration creep stage. Thus, the general trend of the acoustic emission ringing rate in each creep stage is that of "growth–decrease–stability". Additionally, as the water content increases, the ringing rate decreases gradually.

4.4. Changes in the Acoustic Emission Parameters in Creep Deformation

The accumulated acoustic emission ringing counts of the selected specimens and its acoustic emission ringing rate were analyzed for coal samples with different water contents during creep deformation to study the effect of water content on the acoustic emission

parameters during creep deformation of the specimens. The relationship between the creep acoustic emission parameters and strain of the specimens with time under different stress levels can be obtained by incremental loading, as shown in Figure 9.
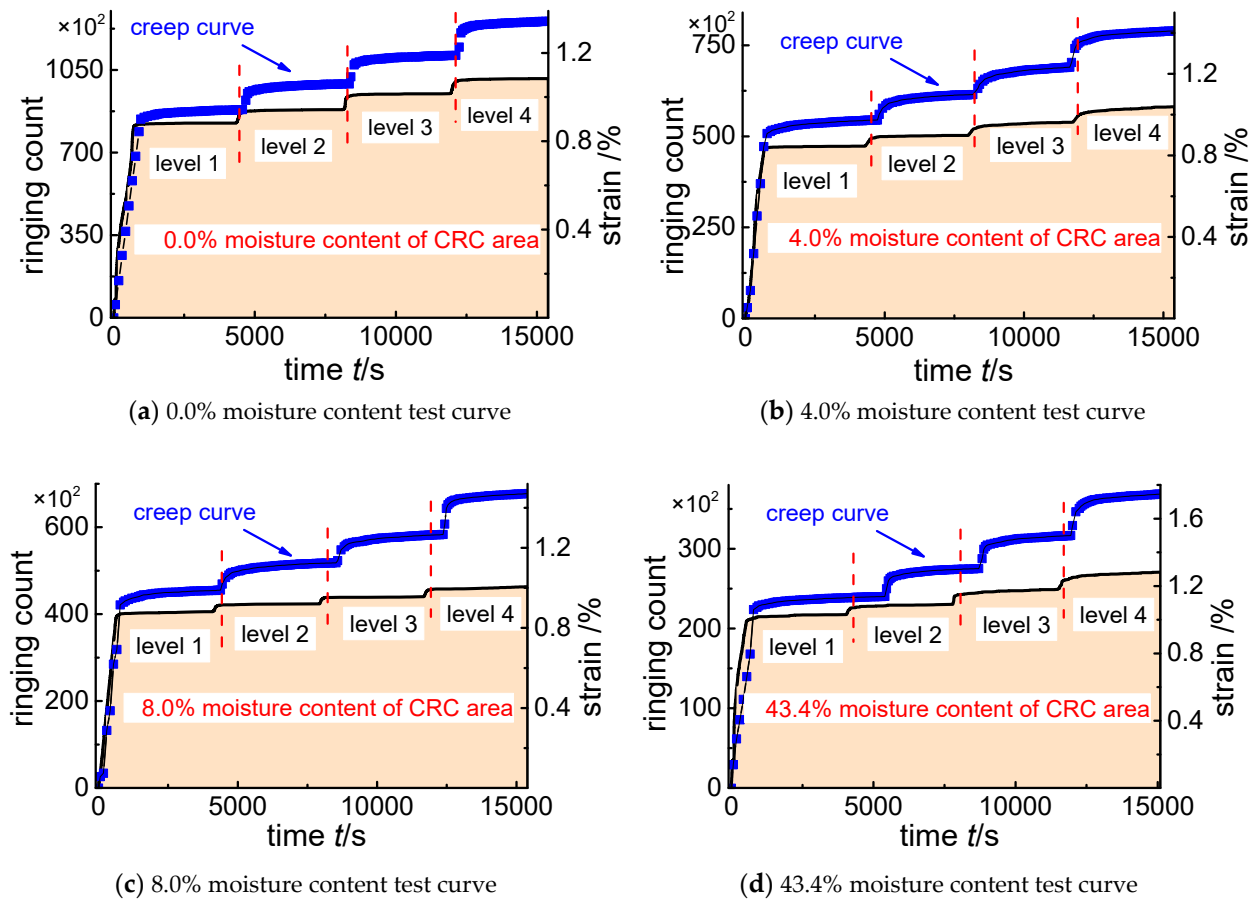

(a) 0.0% moisture content test curve

(b) 4.0% moisture content test curve

(c) 8.0% moisture content test curve

(d) 43.4% moisture content test curve

Figure 9. AE cumulative ringing count (CRC) curve (black line) and creep curve (blue line) with time.

Analysis of Figure 9 can be obtained so that the cumulative acoustic emission ringing counts and creep strain curves of specimens with different moisture contents vary in a pattern, and they all show a trend of higher consistency. That is, when the specimen was in the compression-density stage and when the stress was gradually increased from 0 MPa to the first level of the set stress value (level 1), the accumulated acoustic emission ringing count values were higher for all four water contents. Their cumulative ringing counts accounted for 76–83% of the total value, indicating that there were more ruptures inside the specimen at this stage and the cumulative damage was larger. Subsequently, the cumulative ringing count value increased each time the level of stress increased (level 2–level 4). Once the stress value reached its set level and remained constant, the ringing count also stabilized, resulting in a slow rise in the cumulative acoustic emission ringing count.

In this paper, on the basis of previous studies, the acoustic emission ringing counts and the corresponding variations in the steady-state strain for different stress levels and water contents during graded loading creep were investigated. The results are shown in Table 4.

The analysis revealed that the cumulative ringing count and axial strain generally satisfy the linear relationship.

$$AE = a\varepsilon + b \tag{6}$$

where AE is the cumulative ringing count, ε is the axial strain, and a and b are constants related to the moisture content.

Table 4. AE ringing rate count variations.

Stress Level/%	Water Content/%	Steady-StateStrain/10^{-2}	Increase (+) Decrease (−)/%	Cumulative Ringing Count/10^2	Increase (+) Decrease (−)/%
60	0	1.042	-	878	-
	4	1.075	+3.2	500	−43.1
	8	1.112	+6.7	421	−52.1
	43.4	1.271	+22	228	−73.9
70	0	1.171	-	945	-
	4	1.217	+3.9	535	−43.4
	8	1.234	+5.4	437	−53.8
	43.4	1.475	+25.9	246	−74.3
80	0	1.322	-	1008	-
	4	1.378	+4.2	575	−43.5
	8	1.467	+10.9	461	−54.3
	43.4	1.738	+31.5	268	−74.1

Saturated water-bearing specimens were selected for analysis to study the relationship between cumulative ringing count and axial strain, and the results are shown in Table 5. The parameters were fitted by the least squares method. The correlation coefficient for the saturated specimens was 0.953 while the other three specimen groups had fitting coefficients above 0.95. The relationship between the axial strain of the creep and the cumulative acoustic emission ringing count is basically linear. The slope of the fitted equation decreases with the rising water content. That is, the water content affects both the cumulative ringing count and the magnitude of the axial strain during creep.

Table 5. Relationship between cumulative ringing count and axial strain.

Group	Water Content	Fitting Equation	R^2
A	0.0%	$AE = 1.76 \times 10^3 \varepsilon - 6116$	0.952
B	4.0%	$AE = 1.03 \times 10^3 \varepsilon - 5128$	0.973
C	8.0%	$AE = 6.97 \times 10^2 \varepsilon - 2709$	0.960
D	43.4%	$AE = 3.26 \times 10^2 \varepsilon + 61$	0.953

The reason for this is that water changes the mechanical properties of the coal rock. Water weakens the compressive strength of the coal rock and the cohesive forces between the particles; hence, the coal sample requires less energy for deformation. Therefore, as the water content increases, the acoustic emission activity of the coal samples decreases and the cumulative acoustic emission ring counts decrease, indicating that water has a significant effect on the acoustic emission characteristics of the coal body during creep around the borehole.

5. Conclusions

In this paper, coal bodies with different moisture contents were tested under uniaxial loading and their properties were analyzed. The creep process, strain, and variation of acoustic emission parameters were investigated. The conclusions drawn from the analysis are as follows.

(1) The water content of the coal changes the creep mechanical properties of the coal body around the borehole. With low water content, the change in the strain of the specimen is small; the transient and steady-state strains increase exponentially with rising water content. For the same stress level, the increase of strain in saturated specimens is more significant. At 80% stress level, the transient and steady-state strains of saturated samples increased by 44.5% and 28.6%, respectively, compared with those of dry specimens (0 water content).

(2) The water content affects the cumulative acoustic emission count during creep. The presence of water in the coal affects the values of acoustic emission parameters during

its creep, mainly in terms of cumulative ringing counts and axial strain. The cumulative ringing count of the water-bearing coal samples was 40–80% less than that of the dry coal samples, and the higher the water content, the greater the increase or decrease in the cumulative ringing count.

(3) There are three stages of acoustic emission ringing rate in each creep stage. The acoustic emission ringing count rate showed a pattern of "increase–decrease–stabilize" at each creep stage. As the water content increased, the acoustic emission activity decreased significantly, resulting in a decrease in both the cumulative ringing count and the ringing count rate. The creep curve displayed a time lag with respect to the acoustic emission data.

Author Contributions: The main research idea and manuscript preparation were contributed by T.Z.; Z.L. contributed to the manuscript preparation and performed the correlative experiment. M.P. provided several suggestions from the industrial perspective. Y.M. assisted in finalizing the research and manuscript. All the research in the manuscript complies with ethical requirements and was consented by the participants. All authors have read and agreed to the published version of the manuscript.

Data Availability Statement: The data used to support the findings of this study are available from the corresponding author upon request.

Conflicts of Interest: The authors declare that there is no conflict of interest regarding the publication of this paper.

References

1. Gao, Y.N.; Gao, F.; Ronald, Y.M. Rock creep modeling based on discontinuous deformation analysis. *J. Min. Sci. Technol. Engl.* **2013**, *23*, 757–761. [CrossRef]
2. Liu, L.; Wang, G.M.; Chen, J.H.; Yang, S. Creep experiment and rheological model of deep saturated rock. *Trans. Nonferrous Met. Soc. China* **2013**, *23*, 478–483. [CrossRef]
3. Xiao, H.; Yang, Z.Y.; Cui, Q.L.; Mu, Q.W. Effect of standing water in closed pit mine goaf on the stability of waterproof coal pillar. *Coal Sci. Technol.* **2014**, *4*, 105–107.
4. Hu, K.F.; Feng, Q.; Li, H.; Hu, Q. Study on creep characteristics and constitutive model for Thalam rock mass with fracture in tunnel. *Geotech. Geol. Eng.* **2018**, *36*, 827–834. [CrossRef]
5. Liu, H.Z.; Xie, H.Q.; He, J.D.; Zhuo, L. Nonlinear creep damage constitutive model forsoft rocks. *Mech. Time Depend. Mater.* **2017**, *21*, 73–96. [CrossRef]
6. Yang, S.Q.; Xu, P.; Ranjith, P.G. Damage model of coal under creep and triaxial compression. *Int. J. Rock Mech. Min. Sci.* **2015**, *80*, 337–345. [CrossRef]
7. Jia, Z.; Ren, L.; Liu, Q.; Zha, E. Influence of water-soaking time on the acoustic emission characteristics and spatial fractal dimensions of coal under uniaxial compression. *Therm. Sci.* **2017**, *21*, 327–334. [CrossRef]
8. Ai, T.; Wu, S.; Zhang, R.; Gao, M.; Zhang, Z. Changes in the structure and mechanical properties of a typical coal induced by water immersion. *Int. J. Rock Mech. Min. Sci.* **2021**, *138*, 104597. [CrossRef]
9. Yao, Q.; Zheng, C.; Tang, C.; Li, X. Experimental investigation of the mechanical failure behavior of coal specimens with water intrusion. *Front. Earth Sci.* **2020**, *7*, 348. [CrossRef]
10. Hao, C.; Hou, Z.; Xiao, F.; Liu, G. Experimental Study on influence of borehole arrangement on energy conversion and acoustic characteristics of coal-like material sample. *Shock Vib.* **2020**, *2020*, 1–15. [CrossRef]
11. Liu, R.; He, Y.; Zhao, Y.; Jiang, X.; Ren, S. Statistical analysis of acoustic emission in uniaxial compression of tectonic and non-tectonic coal. *Appl. Sci.* **2020**, *10*, 3555. [CrossRef]
12. Shen, R.; Zhang, X.; Wang, E.; Li, H.; Hou, Z. Application of acoustic emission technique to the evaluation of coal seam hydraulic flushing effect. *Energies* **2019**, *12*, 1705. [CrossRef]
13. Jiang, X.U.; Geng, J.B.; Peng, S.J.; Liu, D.; Nie, W. Acoustic emission characteristics of coal and gas outburst under different moisture contents. *J. China Coal Soc.* **2015**, *2015*, 5.

14. Shen, R.; Li, H.; Wang, E.; Li, D.; Hou, Z.; Zhang, X.; Han, X. Mechanical behavior and AE and EMR characteristics of natural and saturated coal samples in the indirect tensile process. *J. Geophys. Eng.* **2019**, *2019*, 4. [CrossRef]

15. Tang, C.; Yao, Q.; Li, Z.; Zhang, Y.; Ju, M. Experimental study of shear failure and crack propagation in water-bearing coal samples. *Energy Sci. Eng.* **2019**, *7*, 2193–2204. [CrossRef]

16. Chen, T.; Yao, Q.L.; Wei, F.; Zhong, Z.H.; Zhou, J.; Wang, C.B.; Li, J. Effects of water intrusion and loading rate on mechanical properties of and crack propagation in coal-rock combinations. *J. Cent. South Univ.* **2017**, *24*, 423–431. [CrossRef]

17. Qian, R.P.; Feng, G.R.; Guo, J.; Wang, P.; Jiang, H. Effects of water-soaking height on the deformation and failure of coal in uniaxial compression. *Appl. Sci. Base* **2019**, *9*, 4370. [CrossRef]

18. Heggheim, T.; Madland, M.V.; Risnes, R. A chemical induced enhanced weakening of chalk by seawater. *J. Pet. Sci. Eng.* **2014**, *46*, 171–184. [CrossRef]

19. Daraei, A.; Zare, S. Effect of water content variations on critical and failure strains of rock. *KSCE J. Civ. Eng.* **2018**, *22*, 3331–3339. [CrossRef]

20. Qin, H.; Huang, G.; Wang, W.Z. Experimental study on acoustic emission characteristics of compressive deformation and failure of coal rocks with different moisture content. *Chin. J. Rock Mech. Eng.* **2012**, *31*, 1115–1120.

21. Jing, J.J.; Liang, W.G.; Zhang, B.N.; Lu, T.; Xu, J.; Zhang, D.; Huang, G. Experimental study on the influence of water content on gas seepage characteristics of coal seams. *J. Taiyuan Univ. Technol.* **2016**, *47*, 450–454.

22. Wei, J.P.; Qin, H.J.; Wang, D.K.; Jiang, C.B.; Cao, J.; Zhang, Q.G. Study on seepage characteristics of gas-containing coal under loading-unloading confining pressure based on water effect. *J. Min. Saf. Eng.* **2014**, *31*, 987–994.

23. Jiang, C.B.; Duan, M.K.; Yin, G.Z.; Jiang, C.; Qin, H.; Wang, M. Experimental study on loading and unloading of gas-containing raw coal under different water-containing conditions. *J. China Coal Soc.* **2016**, *41*, 2230–2237.

24. Yan, B.; Guo, Q.; Ren, F.; Cai, M. Modified Nishihara model and experimental verification of deep rock mass under the water-rock interaction. *Int. J. Rock Mech. Min. Sci.* **2020**, *128*, 104250. [CrossRef]

25. Ca, O.P.; Wen, Y.; Wang, Y.; Yuan, H.; Yuan, B. Study on nonlinear damage creep constitutive model for high-stress soft rock. *Environ. Earth Sci.* **2016**, *75*, 900. [CrossRef]

26. Tang, H.; Wang, D.; Huang, R.; Pei, X.; Chen, W. A new rock creep model based on variable-order fractional derivatives and continuum damage mechanics. *Bull. Eng. Geol. Environ.* **2018**, *77*, 375–383. [CrossRef]

27. Sun, C.; Li, G.; Gomah, M.E.; Xu, J.; Sun, Y. Creep characteristics of coal and rock investigated by nanoindentation. *Int. J. Min. Sci. Technol.* **2020**, *30*, 769–776. [CrossRef]